Tau PET Imaging in Neurodegenerative Disorders

Colin Groot[1,2], Sylvia Villeneuve[3–5], Ruben Smith[1,6], Oskar Hansson[1,6], and Rik Ossenkoppele[1,2]

[1]Clinical Memory Research Unit, Lund University, Lund, Sweden; [2]Alzheimer Center Amsterdam, Department of Neurology, Amsterdam Neuroscience, Amsterdam UMC, Location VUMC, Amsterdam, The Netherlands; [3]Department of Psychiatry, Faculty of Medicine, McGill University, Montreal, Canada; [4]Douglas Mental Health University Institute, Montreal, Canada; [5]McConnell Brain Imaging Centre, Montreal Neurological Institute, Montreal, Canada; and [6]Memory Clinic, Skåne University Hospital, Malmö, Sweden

The advent of PET ligands that bind tau pathology has enabled the quantification and visualization of tau pathology in aging and in Alzheimer disease (AD). There is strong evidence from neuropathologic studies that the most widely used tau PET tracers (i.e., ^{18}F-flortaucipir, ^{18}F-MK6240, ^{18}F-RO948, and ^{18}F-PI2620) bind tau aggregates formed in AD in the more advanced (i.e., ≥IV) Braak stages. However, tracer binding in most non-AD tauopathies is weaker and overlaps to a large extent with known off-target binding regions, limiting the quantification and visualization of non-AD tau pathology in vivo. Off-target binding is generally present in the substantia nigra, basal ganglia, pituitary, choroid plexus, longitudinal sinuses, meninges, or skull in a tracer-specific manner. Most cross-sectional studies use the inferior aspect of the cerebellar gray matter as a reference region, whereas for longitudinal analyses, an eroded white matter reference region is sometimes selected. No consensus has yet been reached on whether to use partial-volume correction of tau PET data. Although an increased neocortical tau PET signal is rare in cognitively unimpaired individuals, even in amyloid-β–positive cases, such a signal holds important prognostic information because preliminary data suggest that an elevated tau PET signal predicts cognitive decline over time. Also, in symptomatic stages of AD (i.e., mild cognitive impairment or AD dementia), tau PET shows great potential as a prognostic marker because an elevated baseline tau PET retention forecasts future cognitive decline and brain atrophy. For differential diagnostic use, the primary utility of tau PET is to differentiate AD dementia from other neurodegenerative diseases, as is in line with the conditions for the approval of ^{18}F-flortaucipir by the U.S. Food and Drug Administration for clinical use. The differential diagnostic performance drops substantially at the mild-cognitive-impairment stage of AD, and there is no sufficient evidence for detection of sporadic non-AD primary tauopathies at the individual level for any of the currently available tau PET tracers. In conclusion, while the field is currently addressing outstanding methodologic issues, tau PET is gradually moving toward clinical application as a diagnostic and possibly prognostic marker in dementia expert centers and as a tool for selecting participants, assessing target engagement, and monitoring treatment effects in clinical trials.

Key Words: molecular imaging; neurology; PET; Alzheimer; PET; tau; diagnosis; pathology

J Nucl Med 2022; 63:20S–26S
DOI: 10.2967/jnumed.121.263196

Tau is a phosphoprotein that is synthesized throughout the nervous system and is involved in the formation and stabilization of microtubules, which are, in turn, critical for cytoskeletal support and intracellular transport of organelles, secretory vesicles, and neurotransmitters. Tau physiology relies on phosphorylation, but when tau becomes hyperphosphorylated, its normal functionality is altered. Hyperphosphorylation also increases the aggregation of tau into straight filaments, twisted ribbons, or paired helical filaments (*1*). Collectively shared under the rubric of tauopathies, many of the most common neurodegenerative diseases are characterized by tau pathology, such as Alzheimer disease (AD), progressive supranuclear palsy, corticobasal degeneration and Pick disease (*2*). As of 2013, it has been possible to visualize and quantify tau pathology in the living human brain (*3*). Since then, studies using tau PET have shown an exponential rise within the field of neurodegenerative disorders (Fig. 1). To date, a wide array of tracers has been developed, which can roughly be categorized into first-generation and second-generation tau PET tracers. First-generation tau PET tracers include ^{18}F-flortaucipir (also called ^{18}F-T807, ^{18}F-AV1451 and ^{18}F-Tauvid [Eli Lilly and Co.], which is the most widely applied tracer to date), ^{11}C-PBB3, and the ^{18}F-THK family (*4,5*). Second-generation tracers include ^{18}F-MK6240, ^{18}F-RO948, ^{18}F-PI2620, ^{18}F-GTP1, and ^{18}F-JNJ-64326067 (*6–11*) and were developed to minimize the off-target binding observed in the first-generation tau PET tracers.

Most neurodegenerative diseases (including the tauopathies) show a stereotypical distribution of pathology throughout the brain (*10,12*), and PET provides a unique opportunity to provide 3-dimensional topographic images of molecular physiology in the living brain. Therefore, tau PET can serve to detect the presence of a tauopathy in a diagnostic setting and additionally provide valuable information about the spatial patterns of tau pathology. Aside from the promising prospects for tau PET as a diagnostic tool, the strong association between spatial patterns of tau, neurodegeneration, and cognitive impairment (*13–15*) also highlights the potential of tau PET as a prognostic tool. Nearly a decade after the introduction of the first potent tau PET tracer, we will here summarize the current state of the art of the tau PET literature and highlight some of the opportunities and challenges of tau PET. We specifically focus on the neuropathologic correlates of tau PET; methodologic considerations, including on- and off-target binding, PVC, and reference region selection; and finally the potential clinical utility of tau PET in terms of early detection of tau pathology, differential diagnosis of dementia syndromes, and prediction of future rates of cognitive decline across the AD clinical spectrum.

NEUROPATHOLOGIC CORRELATES OF TAU PET SIGNAL

For most established tau PET tracers, there is evidence of binding to the tau aggregates formed in AD (i.e., a mix of 3-repeat

Received Dec. 15, 2021; revision accepted Mar. 9, 2022.
For correspondence or reprints, contact Rik Ossenkoppele (r.ossenkoppele@amsterdamumc.nl).

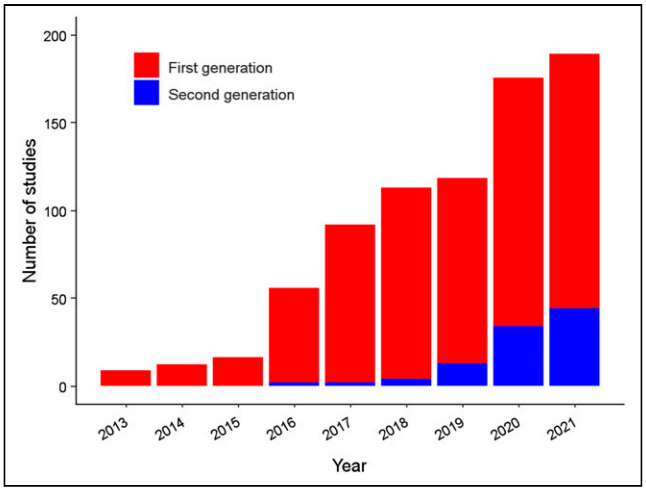

FIGURE 1. Rapid increase in tau PET publications since 2013. Records were obtained from database (https://pubmed.ncbi.nlm.nih.gov/) using search queries for first-generation tau tracers (THK* OR (T807 OR T808 OR AV1451 OR flortaucipir OR Tauvid) OR (PBB3 OR APN1607)) AND (PET OR "positron emission tomography") and for second-generation tau tracers (MK6240 OR (RO948 OR RO69558948) OR PI2620 OR GTP1 OR (JNJ64349311 OR JNJ311 OR JNJ067)) AND (PET OR "positron emission tomography"). Duplicates were not removed to ensure inclusion in both queries for studies that implemented multiple tau tracers.

[3R]/4-repeat [4R] tau isoforms) from autoradiography studies performed on postmortem brain tissue (*16–20*). However, most tracers have shown lower affinity for the 3R and 4R isoforms of tau that characterize many primary tauopathies, possibly related to the lower tau aggregate densities that hamper detection using PET. For ^{18}F-flortaucipir and ^{18}F-MK6240, binding to non-AD tau pathology has been limited according to autoradiography studies, whereas there is some autoradiographic evidence of ^{18}F-PI2620 (*21*) and ^{18}F-PM-PBB3 (a fluorinated version of ^{11}C-PBB3) (*22*) binding to 4R tau inclusions observed in tissue of individuals with progressive supranuclear palsy. To fully validate the radiotracers, it is crucial to verify that the signal detected in vivo corresponds to tau pathology as assessed by postmortem neuropathologic examination of the brain. The most extensive neuropathologic correlations thus far have been performed for ^{18}F-flortaucipir PET (Fig. 2). There is strong evidence, provided by a relatively large end-of-life study (*23*) and extended case series (*24,25*), that ^{18}F-flortaucipir accurately detects AD-like tau neuropathology in individuals in more advanced Braak stages (i.e., Braak > IV; the accuracy for detecting tau load corresponding to Braak stages V and VI was 87.5% [95% CI, 77.2%–93.5%] (*23*)). These data are further supported by the strong correlations (R^2 range, 0.66–0.76) between tau PET levels and the quantitative neuropathologic tau burden in corresponding brain regions (*26,27*). Studies on non-AD tauopathies showed mixed results. In *MAPT*-mutation carriers with mixed 3R/4R tau pathology (akin to AD), there is a strong correspondence (R^2 = 0.86) between the antemortem tau PET scan and the postmortem neuropathologic tau burden (*28,29*). For 4R tauopathies such as progressive supranuclear palsy and corticobasal degeneration, however, the evidence is less clear. Some in vivo signal has been detected in individuals clinically diagnosed with a corticobasal syndrome (*29–31*). However, so far only 5 autopsy-confirmed cases have been published showing either moderate-to-high correlations (R^2 range, 0.59–0.79) of ^{18}F-flortaucipir PET signal with tau pathology (*32,33*) or only minor increases in tracer uptake compared with controls with a limited correlation between the tau PET signal and neuropathology (*24*). There are multiple reports of group-level differences in vivo between controls and clinically diagnosed progressive supranuclear palsy patients using both ^{18}F-flortaucipir (*29,34–36*) and ^{18}F-PI2620 (*21*). Tracer retention is observed mostly in the basal ganglia and substantia nigra, complicating the interpretation because these regions also show off-target binding for several tau PET tracers ("Methodologic Considerations" section). The number of autopsy-confirmed cases is low (*24,37,38*) and demonstrated no correlation between cortical ^{18}F-flortaucipir PET signal and neuropathologic 4R tau (*38*), with little binding outside the off-target regions (*24*). The binding profile of ^{18}F-PI2620 in progressive supranuclear palsy seems more promising, potentially because of lower off-target binding in the basal ganglia. Autoradiography provided some evidence of binding to 4R tau pathology (*21*), but the only neuropathologic correlation study published to date showed limited binding of ^{18}F-PI2620 PET to 4R tau pathology, suggesting that the in vivo tau PET signal only partially reflects postmortem 4R tau pathology (*39*).

In summary, the available neuropathologic data strongly indicate that the current tau PET tracers bind the tau aggregates formed in AD in the more advanced Braak stages (>IV). Tracer binding in most non-AD tauopathies is weaker and overlaps to a large extent with known off-target binding regions, hence limiting

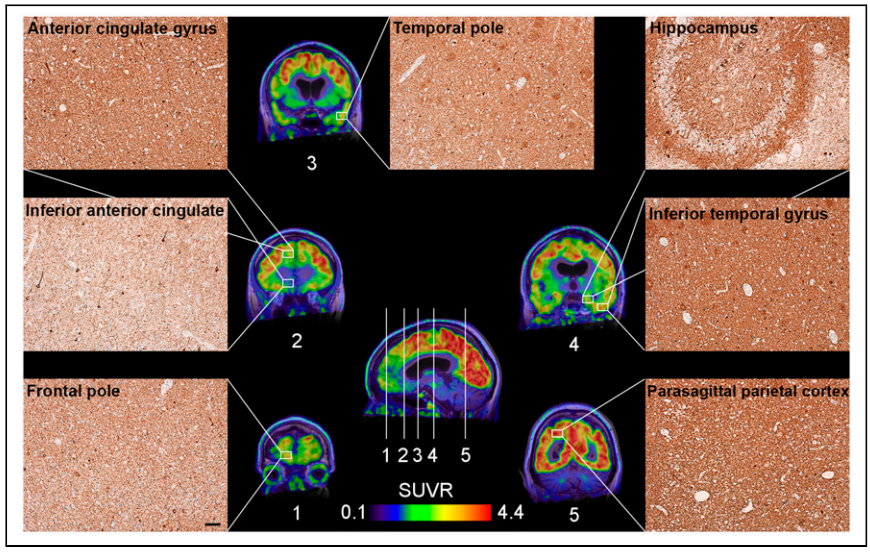

FIGURE 2. Correspondence between neuropathologic tau in comparison to antemortem ^{18}F-flortaucipir PET retention in individual with AD dementia. Depicted are 5 coronal ^{18}F-flortaucipir PET sections labeled as 1 to 5 in anteroposterior direction. Approximate locations of coronal sections are indicated in sagittal section. Corresponding AT8 (phospho-tau) immunohistochemistry images at ×10 magnification were captured from frontal pole, inferior anterior cingulate gyrus, anterior cingulate gyrus, temporal pole, hippocampus, inferior temporal gyrus, and parasagittal parietal cortex. Scale bar = 50 μm.

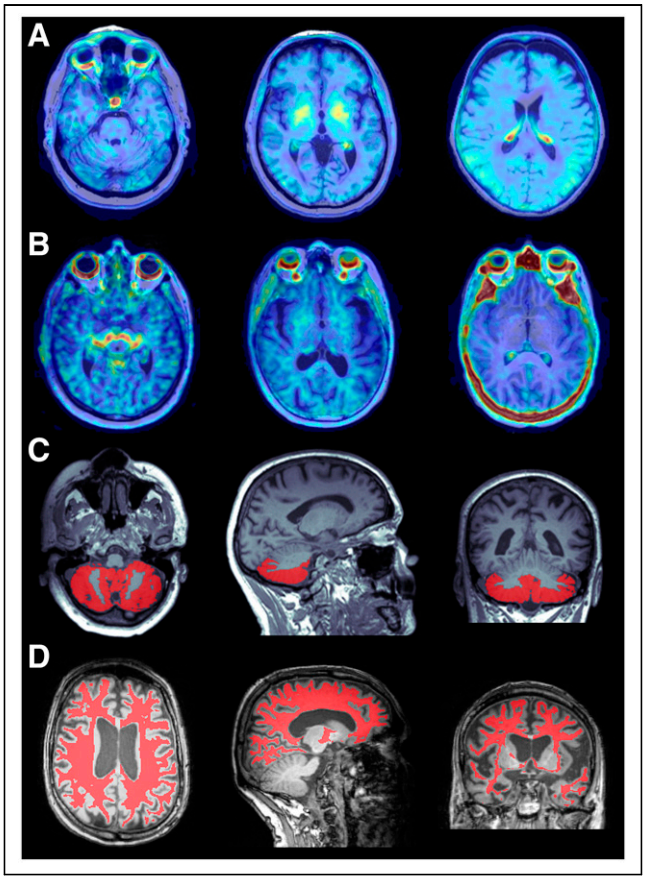

FIGURE 3. (A) ^{18}F-Flortaucipir PET images showing, from left to right (all axial slices), off-target binding in retina and pituitary, basal ganglia, and choroid plexus. (B) ^{18}F-RO948 images showing, from left to right (all axial slices), retinal, substantia nigra, and superior cerebellar off-target binding; retinal off-target binding and notable absence of basal ganglia off-target binding; and extreme case of skull/meningeal off-target binding. (C) Inferior cerebellar reference region. (D) White matter reference region.

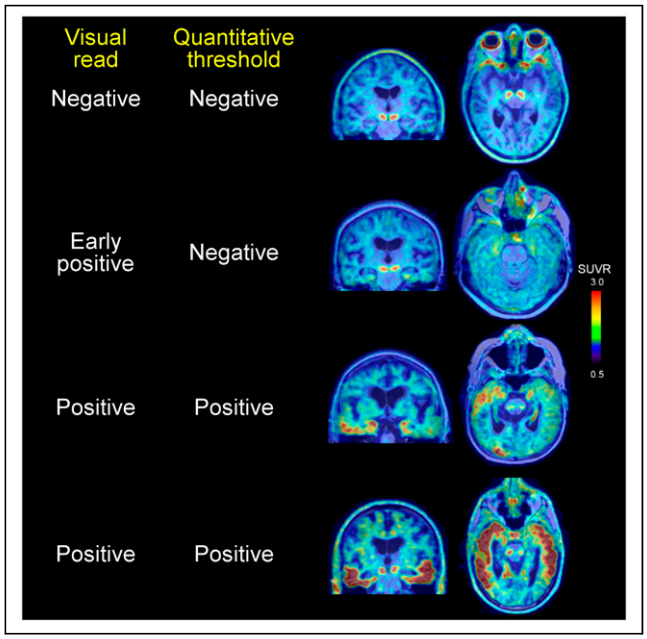

FIGURE 4. Four examples of ^{18}F-RO9848 scans in ascending order of overall tau load, which were evaluated both visually and using quantitative threshold. Second case indicates that visual read can be positive (early) at subthreshold levels of tau PET signal.

the possibility of quantifying and visualizing non-AD tau pathology in vivo.

METHODOLOGIC CONSIDERATIONS OF TAU PET

Off-Target Binding

The off-target binding profile varies widely across tau PET tracers. Some of the first-generation tracers (e.g., ^{11}C-PBB3 and the ^{18}F-THK ligands) show off-target binding to amyloid deposits and monoamine oxidase B to such an extent that it hampers the specificity of these tracers to detect tau pathology (*5*). The most apparent off-target binding targets of ^{18}F-flortaucipir, ^{18}F-RO948, and ^{18}F-MK6240 are neuromelanin in the substantia nigra and retinal pigment epithelium (*17,19,40*). In addition, ^{18}F-flortaucipir shows substantial off-target binding in the basal ganglia, longitudinal sinuses, pituitary, and choroid plexus (Figs 3A–3C), as indicated by head-to-head studies against ^{18}F-RO948 (*41*) and ^{18}F-MK6240 (*42*). In contrast, ^{18}F-RO948 and ^{18}F-MK6240 show greater binding to the meninges and skull (Figs. 3D–3F), especially in women (*43,44*). Only a few reports are available on in vivo off-target binding of ^{18}F-PI2620 to the meninges, skull, and venous sinuses, but published images of the tracer seem to indicate off-target binding to the meninges or skull as well (*39*). Potential sources of the off-target binding across tracers include monoamine oxidase, calcifications, iron, and microhemorrhages (*45*).

PVC

No consensus has yet been reached on the use of partial-volume correction (PVC) in tau PET studies. A recent study assessed 5 different PVC methods and showed that PVC improved the discriminative accuracy between cognitively impaired and unimpaired individuals cross-sectionally but also resulted in less robust longitudinal changes in tau PET signal (*46*). PVC has also been used to reduce the impact of choroid plexus off-target binding on hippocampal signal when using ^{18}F-flortaucipir PET (*47*), but standard (e.g., geometric transfer matrix) and more novel (e.g., Van Cittert iterative deconvolution with highly constrained backprojection denoising) PVC methods only modestly restore hippocampal signal and the correlation between hippocampal signal and clinical symptoms (*48,49*). In our personal experience, although numeric increases in tracer retention are observed in PVC data, the main effects (e.g., cognitive correlates or diagnostic performance) are generally highly similar with and without PVC. Still, in relevant scenarios (e.g., in longitudinal settings or in the presence of marked brain atrophy), we recommend reporting results both with and without PVC.

Reference Region Selection

The most widely used reference region for tau PET studies is the cerebellar gray matter. This region is devoid of tau in neuropathologic studies (*27*) and shows low variance in amyloid-β–negative controls (*45*). Preferentially, the inferior cerebellar cortex or cerebellar crus, corresponding to the mid portion of the cerebellar gray matter, has been used to minimize spill-in from occipital lobe signal and to avoid off-target binding in the superior parts of the cerebellar vermis observed with some tracers (*47*). Recent studies indicate that an inferior cerebellar reference region provided the most sensitive measure for cross-sectional group differences (*50*), whereas an eroded white matter or an eroded white matter cerebellar composite reference region in conjunction with a dedicated longitudinal processing pipeline is most suitable for longitudinal

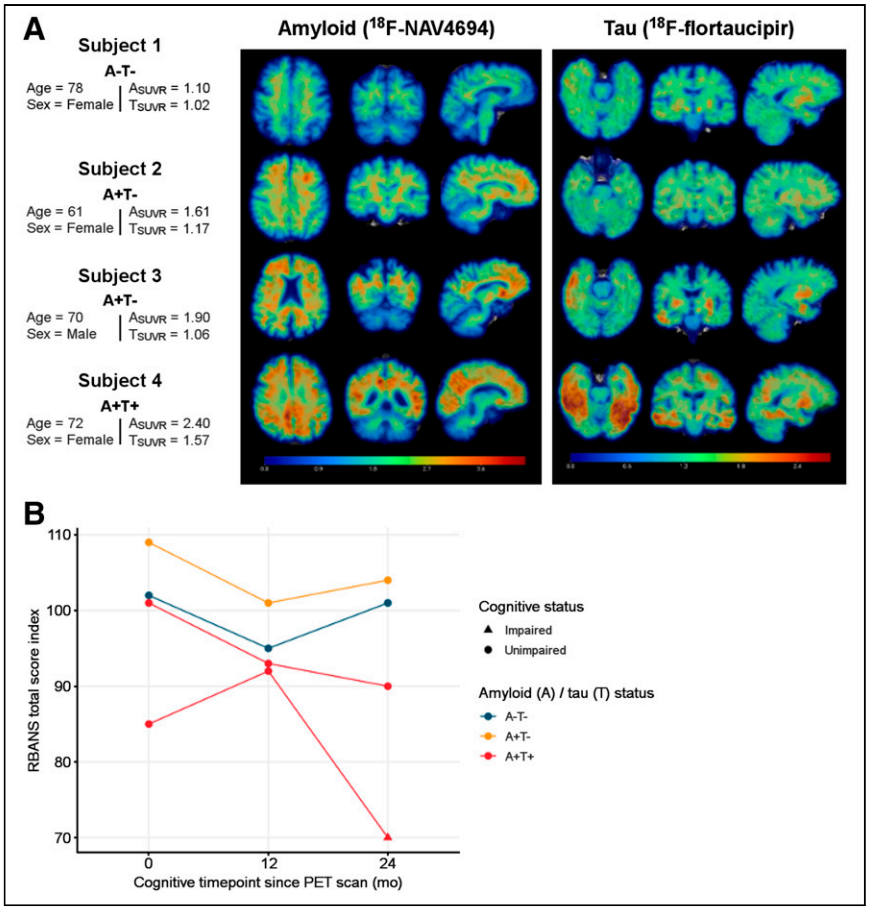

FIGURE 5. (A) Scans of 4 representative participants with different amyloid and tau profiles. One participant was negative on both biomarkers, 2 participants were positive on amyloid only, and 1 participant was positive on both amyloid and tau PET. Global amyloid level (NAV4694; global brain threshold of ≥1.29 SUVR; cerebellar cortex as reference region) and bilateral entorhinal cortex tau level (flortaucipir; bilateral entorhinal cortex of ≥1.23 SUVR; inferior cerebellum as reference region) were used to determine biomarker status. A_{SUVR} and T_{SUVR} represent values averaged across neocortical regions. (B) Prospective cognitive trajectories on RBANS total score index for each of the 4 participants. RBANS = Repeatable Battery for Assessment of Neuropsychological Status.

analyses (*46,50,51*). The latter will need to be verified in samples that contain more individuals with a high cortical tau burden, given the risk of spill-in due to the close proximity between a white matter reference region and the cortex.

Determining Tau PET Positivity

There is currently no consensus on how to define tau PET positivity, thus hampering comparisons between studies. Positivity on a tau PET scan has been characterized by use of quantitative thresholds and visual assessment (*52*). Both require a selection of brain regions in which positivity will be determined. This selection of regions may differ between early stages (e.g., entorhinal cortex) and later stages (e.g., temporoparietal cortex) of AD. The binary classification of tau PET scans is further influenced by the methodologic approach to define a quantitative threshold (e.g., a gaussian mixture modeling or taking the 90th percentile in amyloid-β–negative cognitively unimpaired individuals) and the visual read procedures (53). This is particularly pertinent to early disease stages, when the signal-to-noise ratio is often low. Several regions of interest have been proposed as potential candidates to detect early tau accumulation. The entorhinal or transentorhinal cortex is usually considered the earliest region in which tau PET tracers can detect tau pathology and is therefore often used to define tau PET abnormality at the preclinical disease stage. However, tau pathology in the entorhinal cortex might not be specific to AD since autopsy studies have shown that entorhinal tau pathology commonly occurs in older individuals without amyloid-β pathology in a condition referred to as primary age-related tauopathy (*54*). An alternative approach is to use a temporal meta–region of interest (ROI) consisting of the entorhinal, fusiform, and inferior and middle temporal cortices; the amygdala; and the parahippocampus. This ROI has the advantage of being more specific to AD, although at the expense of its sensitivity in early stages because only a small proportion (5%–10%) of amyloid-β–positive cognitively unimpaired individuals is quantitatively classified as tau PET–positive in this ROI (*55,56*). Another advantage of the temporal meta-ROI (or temporoparietal cortex) is that it optimally captures the heterogeneous distribution of tau pathology across both typical presentations (i.e., ∼70% conforms to the traditional Braak staging scheme of neurofibrillary tangle pathology) and atypical presentations (e.g., posterior cortical atrophy ["visual AD"] and logopenic variant primary progressive aphasia ["language AD"]) of AD (*57,58*). Importantly, visual assessment of mild temporal binding has been found to enhance sensitivity in detecting tau in early disease stages when compared with temporal meta-ROI quantification (Fig. 4) (*59*). When comparing visually versus quantitatively discordant tau PET status, visual assessment yielded the highest rate of tau PET positivity. Despite the fact that they did not reach the SUV ratio (SUVR) threshold for positivity, isolated visually positive individuals also showed elevated amyloid PET positivity, cerebrospinal fluid phosphorylated-tau 181 concentrations, and tau PET SUVRs.

CLINICAL USE OF TAU PET

Early Detection

In the past few decades, amyloid PET has been the imaging modality of choice for early detection of AD. Amyloid-β pathology, however, is highly prevalent among older adults, and although the presence of amyloid-β is necessary for a diagnosis of AD, it might not be sufficient to cause clinical AD (*60*). Furthermore, individuals with amyloidosis can remain cognitively normal for decades before they start experiencing cognitive symptoms, making amyloid-β a suboptimal predictor of clinical progression in cognitively unimpaired individuals. To improve the identification of individuals with early AD in a research setting, the amyloid-β (A), tau (T), and neurodegeneration (N) framework has been proposed (*61*). This biologic framework is especially useful for individuals that are not yet

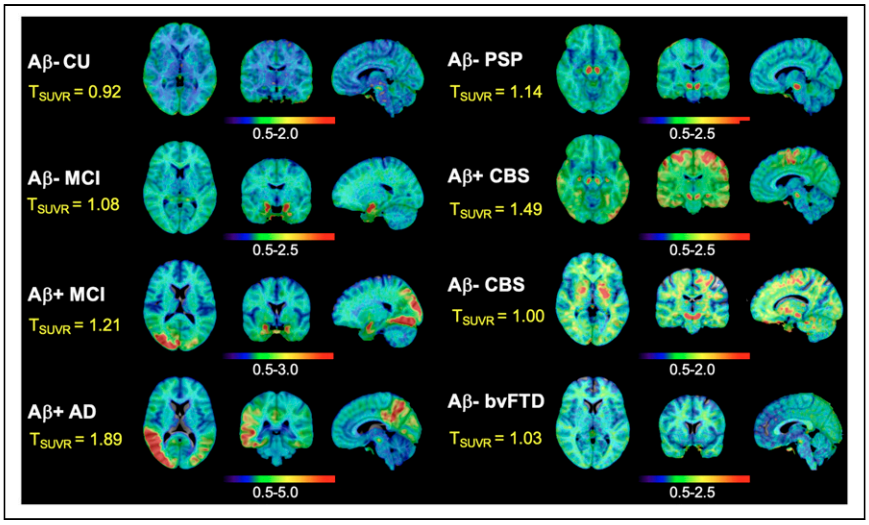

FIGURE 6. Examples of representative tau PET scans across different diagnostic groups. All PET scans were obtained 70–90 min after injection of 370 MBq of ^{18}F-RO948 on GE Healthcare Discovery scanner, projected onto coregistered T1-weighted MRI scan, normalized to standard MNI space, and finally converted to SUVRs using inferior cerebellar cortex as reference tissue. Scans were obtained from BioFINDER-2 cohort. Color scales indicate SUVRs and are individually tailored to best visualize tau PET patterns across different diagnoses. T_{SUVR} represents average uptake in late-stage (Braak V–VI) tau regions. All slices are depicted in radiologic convention. Aβ = amyloid β; bvFTD = behavioral variant of frontotemporal dementia; CBS = corticobasal syndrome; CU = cognitively unimpaired; MCI = mild cognitive impairment; PSP = progressive supranuclear palsy.

experiencing the clinical consequences of the disease. One challenge, however, is that it requires continuous biologic variables to be dichotomized into binary categoric classifications. Although a global measure can be used for defining amyloid PET positivity given the already widespread distribution of amyloid-β pathology in early stages, such is not the case for tau PET because tau pathology in the neocortex manifests closer to symptomatic stages of the disease and requires a more refined regional approach.

Given its high specificity, tau PET quantification has been found to be superior to amyloid PET and MRI in predicting preclinical and prodromal cognitive changes (*62*). In the PREVENT-AD study ("Presymptomatic Evaluation of Experimental or Novel Treatments for Alzheimer Disease"), 129 cognitively unimpaired participants (mean age, 67 y [SD, 5 y]) underwent amyloid and tau PET scans and were subsequently followed for a minimum of 2 y (*63*). Both increased amyloid and tau PET levels were associated with cognitive decline, but this relationship was predominantly driven by tau (i.e., when both amyloid and tau were included in the model, only tau remained significant). Figure 5A shows representative examples of amyloid and tau PET scans of 4 PREVENT-AD participants who were cognitively unimpaired at the time of these PET scans. Figure 5B shows the cognitive trajectory of these same individuals over the course of 2 y. Although both the A-negative, T-negative participant and the A-positive, T-negative participant remained cognitively unimpaired over the course of the follow-up, the A-positive, T-positive participants demonstrated cognitive decline, and one of them even met diagnostic criteria for mild cognitive impairment at the 2-y follow-up visit. Only one participant was classified as A-negative, T-positive; this participant was cognitively stable over time. In summary, T positivity, especially in combination with A positivity, seems to be a key driver of cognitive decline. Tau PET positivity could therefore be an excellent marker to predict short-term progression from cognitive nonimpairment to mild cognitive impairment in participants at risk of AD dementia.

Prognosis in Symptomatic AD

In symptomatic stages of AD (i.e., mild cognitive impairment and AD dementia), elevated amyloid and tau PET levels at baseline are strongly associated with a more rapid cognitive decline (*62,64,65*) and outperformed amyloid PET and structural MRI measures in head-to-head comparisons (*62,66*). Furthermore, among participants with mild cognitive impairment and AD dementia, a visually determined positive ^{18}F-flortaucipir PET scan was associated with an increased risk for future cognitive decline (Mini-Mental State Examination hazard ratio, 1.68 [95% CI, 1.22–2.32]) and functional decline (CDR sum of boxes hazard ratio, 1.40 [95% CI, 1.11–1.76]) after 18 mo of follow-up (*67*). Both the intensity and the extent of baseline tau PET levels were also strongly predictive for future rates of brain atrophy among participants with mild cognitive impairment and AD dementia (*68*). In summary, tau PET shows great potential as a prognostic marker in symptomatic stages of AD.

Differential Diagnosis

Differentiating between neurodegenerative diseases is challenging because clinical presentations and patterns of neurodegeneration can substantially overlap across disorders. Given that most neurodegenerative dementias are characterized by tauopathy, it has been estimated that, when correctly implemented, tau PET imaging may be able to detect up to 70% of neurodegenerative dementias in a diagnostic setting (*69*). The most established tau PET tracers (i.e., ^{18}F-flortaucipir, ^{18}F-MK6240, and ^{18}F-RO948) have demonstrated excellent diagnostic performance for distinguishing AD dementia from non-AD neurodegenerative disorders, with a sensitivity and specificity above 90% (*56,70,71*). Some exemplary BioFINDER-2 ("Biomarkers for Identifying Neurodegenerative Disorders Early and Reliably") cases with ^{18}F-RO948 PET are shown in Figure 6. In this regard, tau PET is superior to other AD biomarkers, including structural MRI, amyloid-β PET, and most biofluid markers (*56,72–74*). Furthermore, tau PET can be helpful in accurately detecting atypical (nonamnestic) variants of AD, which show highly distinct patterns of tau pathology compared with typical (amnestic-predominant) AD cases (*75,76*). There are several remaining challenges for the use of tau PET in the clinic as a differential diagnostic tool. First, the discriminative accuracy of tau PET tracers drops substantially at the prodromal stage of AD, hence making it most suitable for use in more advanced (i.e., dementia) stages of AD (*56,77,78*). Second, although tau PET tracers are often capable of differentiating non-AD tauopathies such as progressive supranuclear palsy, corticobasal degeneration, and Pick disease from controls at a group level, their utility at an individual-patient level is limited ("Methodologic Considerations" section). Third, it will be important to understand why we commonly observe elevated tau PET signal in clinical syndromes

that are typically not associated with tau pathology, such as the semantic variant of primary progressive aphasia (*79,80*), which in most cases is caused by TDP-43 type C pathology. In summary, in line with the conditions of the approval of ^{18}F-flortaucipir by the U.S. Food and Drug Administration, the current diagnostic utility of tau PET is mainly to differentiate AD dementia from other neurodegenerative diseases (*81*).

CONCLUSIONS AND FUTURE DIRECTIONS

There is strong evidence from neuropathologic studies that the most widely used tau PET tracers (i.e., ^{18}F-flortaucipir, ^{18}F-MK6240, ^{18}F-RO948, and ^{18}F-PI2620) bind tau aggregates formed in AD in the more advanced Braak stages. However, tracer binding in most non-AD tauopathies is weaker and overlaps to a large extent with known off-target binding regions, hence limiting the possibility of quantifying and visualizing non-AD tau pathology in vivo. All tau PET tracers are characterized by off-target binding, and the application of PVC methods and selection of the optimal reference region for longitudinal studies are currently being refined. Tau PET has shown excellent diagnostic accuracy for distinguishing AD dementia from non-AD neurodegenerative disorders and has shown promise for early detection of AD among cognitively unimpaired individuals and for prognostic use in symptomatic stages of AD. Important next steps for the tau PET field include developing appropriate-use criteria akin to those for amyloid PET (*82*), investigating the diagnostic and prognostic value of tau PET in older and ethnically more diverse populations, performing head-to-head comparisons against cerebrospinal fluid and plasma biomarkers of AD pathology (e.g., p-tau and the $A\beta_{42-40}$ ratio) and neurodegeneration (e.g., neurofilament light chain and glial fibrillary acidic protein), determining the long-term cognitive consequences of being exposed to neocortical tau pathology in cognitively unimpaired individuals, and refining tau PET measures for participant selection, target engagement, and treatment monitoring in clinical trials.

DISCLOSURE

Oskar Hansson has acquired research support (for the institution) from AVID Radiopharmaceuticals, Biogen, Eli Lilly, Eisai, GE Healthcare, Pfizer, and Roche. In the past 2 years, he has received consultancy or speaker fees from Roche, Genentech, Siemens, Biogen, Alzpath, and Cerveau. No other potential conflict of interest relevant to this article was reported.

REFERENCES

1. Buée L, Bussière T, Buée-Scherrer V, Delacourte A, Hof PR. Tau protein isoforms, phosphorylation and role in neurodegenerative disorders. *Brain Res Brain Res Rev.* 2000;33:95–130.
2. Lee VMY, Goedert M, Trojanowski JQ. Neurodegenerative tauopathies. *Annu Rev Neurosci.* 2001;24:1121–1159.
3. Chien DT, Bahri S, Szardenings AK, et al. Early clinical PET imaging results with the novel PHF-tau radioligand [F-18]-T807. *J Alzheimers Dis.* 2013;34:457–468.
4. Wolters EE, Dodich A, Boccardi M, et al. Clinical validity of increased cortical uptake of [^{18}F]flortaucipir on PET as a biomarker for Alzheimer's disease in the context of a structured 5-phase biomarker development framework. *Eur J Nucl Med Mol Imaging.* 2021;48:2097–2109.
5. Chiotis K, Dodich A, Boccardi M, et al. Clinical validity of increased cortical binding of tau ligands of the THK family and PBB3 on PET as biomarkers for Alzheimer's disease in the context of a structured 5-phase development framework. *Eur J Nucl Med Mol Imaging.* 2021;48:2086–2096.
6. Maruyama M, Shimada H, Suhara T, et al. Imaging of tau pathology in a tauopathy mouse model and in Alzheimer patients compared to normal controls. *Neuron.* 2013;79:1094–1108.
7. Mattsson N, Schöll M, Strandberg O, et al. ^{18}F-AV-1451 and CSF T-tau and P-tau as biomarkers in Alzheimer's disease. *EMBO Mol Med.* 2017;9:1212–1223.
8. Gobbi LC, Knust H, Körner M, et al. Identification of three novel radiotracers for imaging aggregated tau in Alzheimer's disease with positron emission tomography. *J Med Chem.* 2017;60:7350–7370.
9. Declercq L, Rombouts F, Koole M, et al. Preclinical Evaluation of ^{18}F-JNJ64349311, a novel PET tracer for tau imaging. *J Nucl Med.* 2017;58:975–981.
10. Aguero C, Dhaynaut M, Normandin MD, et al. Autoradiography validation of novel tau PET tracer [F-18]-MK-6240 on human postmortem brain tissue. *Acta Neuropathol Commun.* 2019;7:37.
11. Bischof GN, Dodich A, Boccardi M, et al. Clinical validity of second-generation tau PET tracers as biomarkers for Alzheimer's disease in the context of a structured 5-phase development framework. *Eur J Nucl Med Mol Imaging.* 2021;48:2110–2120.
12. Williams DR, Holton JL, Strand C, et al. Pathological tau burden and distribution distinguishes progressive supranuclear palsy-parkinsonism from Richardson's syndrome. *Brain.* 2007;130:1566–1576.
13. Arriagada PV, Growdon JH, Hedley-Whyte ET, Hyman BT. Neurofibrillary tangles but not senile plaques parallel duration and severity of Alzheimer's disease. *Neurology.* 1992;42:631–639.
14. Nelson PT, Alafuzoff I, Bigio EH, et al. Correlation of Alzheimer disease neuropathologic changes with cognitive status: a review of the literature. *J Neuropathol Exp Neurol.* 2012;71:362–381.
15. Spires-Jones TL, Hyman BT. The intersection of amyloid beta and tau at synapses in Alzheimer's disease. *Neuron.* 2014;82:756–771.
16. Lowe VJ, Curran G, Fang P, et al. An autoradiographic evaluation of AV-1451 tau PET in dementia. *Acta Neuropathol Commun.* 2016;4:58.
17. Marquié M, Normandin MD, Vanderburg CR, et al. Validating novel tau positron emission tomography tracer [F-18]-AV-1451 (T807) on postmortem brain tissue. *Ann Neurol.* 2015;78:787–800.
18. Sander K, Lashley T, Gami P, et al. Characterization of tau positron emission tomography tracer [^{18}F]AV-1451 binding to postmortem tissue in Alzheimer's disease, primary tauopathies, and other dementias. *Alzheimers Dement.* 2016;12:1116–1124.
19. Aguero C, Dhaynaut M, Normandin MD, et al. Autoradiography validation of novel tau PET tracer [F-18]-MK-6240 on human postmortem brain tissue. *Acta Neuropathol Commun.* 2019;7:37.
20. Leuzy A, Chiotis K, Lemoine L, et al. Tau PET imaging in neurodegenerative tauopathies: still a challenge. *Mol Psychiatry.* 2019;24:1112–1134.
21. Brendel M, Barthel H, van Eimeren T, et al. Assessment of ^{18}F-PI-2620 as a biomarker in progressive supranuclear palsy. *JAMA Neurol.* 2020;77:1408–1419.
22. Tagai K, Ono M, Kubota M, et al. High-contrast in vivo imaging of tau pathologies in Alzheimer's and non-Alzheimer's disease tauopathies. *Neuron.* 2021;109:42–58.e48.
23. Fleisher AS, Pontecorvo MJ, Devous MD Sr, et al. Positron emission tomography imaging with [^{18}F]flortaucipir and postmortem assessment of Alzheimer disease neuropathologic changes. *JAMA Neurol.* 2020;77:829–839.
24. Soleimani-Meigooni DN, Iaccarino L, La Joie R, et al. ^{18}F-flortaucipir PET to autopsy comparisons in Alzheimer's disease and other neurodegenerative diseases. *Brain.* 2020;143:3477–3494.
25. Lowe VJ, Lundt ES, Albertson SM, et al. Tau-positron emission tomography correlates with neuropathology findings. *Alzheimers Dement.* 2020;16:561–571.
26. Pontecorvo MJ, Keene CD, Beach TG, et al. Comparison of regional flortaucipir PET with quantitative tau immunohistochemistry in three subjects with Alzheimer's disease pathology: a clinicopathological study. *EJNMMI Res.* 2020;10:65.
27. Smith R, Wibom M, Pawlik D, Englund E, Hansson O. Correlation of in vivo [^{18}F]flortaucipir with postmortem Alzheimer disease tau pathology. *JAMA Neurol.* 2019;76:310–317.
28. Smith R, Puschmann A, Scholl M, et al. ^{18}F-AV-1451 tau PET imaging correlates strongly with tau neuropathology in MAPT mutation carriers. *Brain.* 2016;139:2372–2379.
29. Tsai RM, Bejanin A, Lesman-Segev O, et al. ^{18}F-flortaucipir (AV-1451) tau PET in frontotemporal dementia syndromes. *Alzheimers Res Ther.* 2019;11:13.
30. Cho H, Baek MS, Choi JY, et al. ^{18}F-AV-1451 binds to motor-related subcortical gray and white matter in corticobasal syndrome. *Neurology.* 2017;89:1170–1178.
31. Smith R, Scholl M, Widner H, et al. In vivo retention of ^{18}F-AV-1451 in corticobasal syndrome. *Neurology.* 2017;89:845–853.
32. Josephs KA, Whitwell JL, Tacik P, et al. [^{18}F]AV-1451 tau-PET uptake does correlate with quantitatively measured 4R-tau burden in autopsy-confirmed corticobasal degeneration. *Acta Neuropathol (Berl).* 2016;132:931–933.
33. McMillan CT, Irwin DJ, Nasrallah I, et al. Multimodal evaluation demonstrates in vivo ^{18}F-AV-1451 uptake in autopsy-confirmed corticobasal degeneration. *Acta Neuropathol (Berl).* 2016;132:935–937.
34. Cho H, Choi JY, Hwang MS, et al. Subcortical ^{18}F-AV-1451 binding patterns in progressive supranuclear palsy. *Mov Disord.* 2017;32:134–140.

35. Smith R, Schain M, Nilsson C, et al. Increased basal ganglia binding of ^{18}F-AV-1451 in patients with progressive supranuclear palsy. *Mov Disord.* 2017;32: 108–114.
36. Whitwell JL, Lowe VJ, Tosakulwong N, et al. [^{18}F]AV-1451 tau positron emission tomography in progressive supranuclear palsy. *Mov Disord.* 2017;32:124–133.
37. Smith R, Pawlik D, Nilsson CF, Englund E, Hansson O. [^{18}F]flortaucipir distinguishes Alzheimer's disease from progressive supranuclear palsy pathology in a mixed-pathology case. *Acta Neuropathol (Berl).* 2020;139:411–413.
38. Smith R, Scholl M, Honer M, Nilsson CF, Englund E, Hansson O. Tau neuropathology correlates with FDG-PET, but not AV-1451-PET, in progressive supranuclear palsy. *Acta Neuropathol (Berl).* 2017;133:149–151.
39. Tezuka T, Takahata K, Seki M, et al. Evaluation of [^{18}F]PI-2620, a second-generation selective tau tracer, for assessing four-repeat tauopathies. *Brain Commun.* 2021;3(4):fcab190.
40. Hansen AK, Damholdt MF, Fedorova TD, et al. In vivo cortical tau in Parkinson's disease using ^{18}F-AV-1451 positron emission tomography. *Mov Disord.* 2017;32: 922–927.
41. Smith R, Scholl M, Leuzy A, et al. Head-to-head comparison of tau positron emission tomography tracers [^{18}F]flortaucipir and [^{18}F]RO948. *Eur J Nucl Med Mol Imaging.* 2020;47:342–354.
42. Gogola A, Minhas DS, Villemagne VL, et al. Direct comparison of the tau PET tracers [^{18}F]flortaucipir and [^{18}F]MK-6240 in human subjects. *J Nucl Med.* 2022; 63:108–116.
43. Betthauser TJ, Cody KA, Zammit MD, et al. In vivo characterization and quantification of neurofibrillary tau PET radioligand ^{18}F-MK-6240 in humans from Alzheimer disease dementia to young controls. *J Nucl Med.* 2019;60:93–99.
44. Smith R, Strandberg O, Leuzy A, et al. Sex differences in off-target binding using tau positron emission tomography. *Neuroimage Clin.* 2021;31:102708.
45. Baker SL, Harrison TM, Maass A, La Joie R, Jagust WJ. Effect of off-target binding on ^{18}F-flortaucipir variability in healthy controls across the life span. *J Nucl Med.* 2019;60:1444–1451.
46. Schwarz CG, Therneau TM, Weigand SD, et al. Selecting software pipelines for change in flortaucipir SUVR: balancing repeatability and group separation. *Neuroimage.* 2021;238:118259.
47. Baker SL, Maass A, Jagust WJ. Considerations and code for partial volume correcting [^{18}F]-AV-1451 tau PET data. *Data Brief.* 2017;15:648–657.
48. Pawlik D, Leuzy A, Strandberg O, Smith R. Compensating for choroid plexus based off-target signal in the hippocampus using ^{18}F-flortaucipir PET. *Neuroimage.* 2020;221:117193.
49. Wolters EE, Ossenkoppele R, Golla SS, et al. Hippocampal [^{18}F]flortaucipir BPND corrected for possible spill-in of the choroid plexus retains strong clinicopathological relationships. *Neuroimage Clin.* 2020;25:102113.
50. Young CB, Landau SM, Harrison TM, Poston KL, Mormino EC; ADNI. Influence of common reference regions on regional tau patterns in cross-sectional and longitudinal [^{18}F]-AV-1451 PET data. *Neuroimage.* 2021;243:118553.
51. Southekal S, Devous MD Sr, Kennedy I, et al. Flortaucipir F18 quantitation using parametric estimation of reference signal intensity. *J Nucl Med.* 2018;59: 944–951.
52. Villemagne VL, Lopresti BJ, Dore V, et al. What is T+? A Gordian knot of tracers, thresholds, and topographies. *J Nucl Med.* 2021;62:614–619.
53. Maass A, Landau S, Baker SL, et al. Comparison of multiple tau-PET measures as biomarkers in aging and Alzheimer's disease. *Neuroimage.* 2017;157:448–463.
54. Crary JF, Trojanowski JQ, Schneider JA, et al. Primary age-related tauopathy (PART): a common pathology associated with human aging. *Acta Neuropathol (Berl).* 2014;128:755–766.
55. Ossenkoppele R, Jansen WJ, Rabinovici GD, et al. Prevalence of amyloid PET positivity in dementia syndromes: a meta-analysis. *JAMA.* 2015;313: 1939–1949.
56. Ossenkoppele R, Rabinovici GD, Smith R, et al. Discriminative accuracy of [^{18}F]flortaucipir positron emission tomography for Alzheimer disease vs other neurodegenerative disorders. *JAMA.* 2018;320:1151–1162.
57. Ossenkoppele R, Schonhaut DR, Scholl M, et al. Tau PET patterns mirror clinical and neuroanatomical variability in Alzheimer's disease. *Brain.* 2016;139:1551–1567.
58. Vogel JW, Young AL, Oxtoby NP, et al. Four distinct trajectories of tau deposition identified in Alzheimer's disease. *Nat Med.* 2021;27:871–881.
59. Provost K, Iaccarino L, Soleimani-Meigooni DN, et al. Comparing ATN-T designation by tau PET visual reads, tau PET quantification, and CSF PTau181 across three cohorts. *Eur J Nucl Med Mol Imaging.* 2021;48:2259–2271.
60. Small SA, Duff K. Linking Abeta and tau in late-onset Alzheimer's disease: a dual pathway hypothesis. *Neuron.* 2008;60:534–542.
61. Jack CR Jr, Bennett DA, Blennow K, et al. NIA-AA research framework: toward a biological definition of Alzheimer's disease. *Alzheimers Dement.* 2018; 14:535–562.
62. Ossenkoppele R, Smith R, Mattsson-Carlgren N, et al. Accuracy of tau positron emission tomography as a prognostic marker in preclinical and prodromal Alzheimer disease. *JAMA Neurol.* 2021;78:961–971.
63. Pichet Binette A, Vachon-Presseau E, Morris J, et al. Amyloid and tau pathology associations with personality traits, neuropsychiatric symptoms, and cognitive lifestyle in the preclinical phases of sporadic and autosomal dominant Alzheimer's disease. *Biol Psychiatry.* 2021;89:776–785.
64. Cho H, Choi JY, Lee HS, et al. Progressive tau accumulation in Alzheimer disease: 2-year follow-up study. *J Nucl Med.* 2019;60:1611–1621.
65. Pontecorvo MJ, Devous MD, Kennedy I, et al. A multicentre longitudinal study of (^{18}F)flortaucipir in normal ageing, mild cognitive impairment and Alzheimer's disease dementia. *Brain.* 2019;142:1723–1735.
66. Biel D, Brendel M, Rubinski A, et al. Tau-PET and in vivo Braak-staging as prognostic markers of future cognitive decline in cognitively normal to demented individuals. *Alzheimers Res Ther.* 2021;13:137.
67. Lu M, Pontecorvo MJ, Devous MD Sr, et al. Aggregated tau measured by visual interpretation of flortaucipir positron emission tomography and the associated risk of clinical progression of mild cognitive impairment and Alzheimer disease: results from 2 phase III clinical trials. *JAMA Neurol.* 2021;78:445–453.
68. La Joie R, Visani AV, Baker SL, et al. Prospective longitudinal atrophy in Alzheimer's disease correlates with the intensity and topography of baseline tau-PET. *Sci Transl Med.* 2020;12:eaau5732.
69. Higuchi M. Tau PET imaging. *Adv Exp Med Biol.* 2019;1184:217–230.
70. Jack CR, Wiste HJ, Botha H, et al. The bivariate distribution of amyloid-β and tau: relationship with established neurocognitive clinical syndromes. *Brain.* 2019;142: 3230–3242.
71. Leuzy A, Pascoal TA, Strandberg O, et al. A multicenter comparison of [^{18}F]flortaucipir, [^{18}F]RO948, and [^{18}F]MK6240 tau PET tracers to detect a common target ROI for differential diagnosis. *Eur J Nucl Med Mol Imaging.* 2021;48:2295–2305.
72. Mattsson N, Smith R, Strandberg O, et al. Comparing ^{18}F-AV-1451 with CSF t-tau and p-tau for diagnosis of Alzheimer disease. *Neurology.* 2018;90:e388–e395.
73. Leuzy A, Smith R, Ossenkoppele R, et al. Diagnostic performance of F18-RO948 tau positron emission tomography in the differentiation of Alzheimer disease from other neurodegenerative disorders. *JAMA Neurol.* 2020;77:955–965.
74. Palmqvist S, Janelidze S, Quiroz YT, et al. Discriminative accuracy of plasma phospho-tau217 for Alzheimer disease vs other neurodegenerative disorders. *JAMA.* 2020;324:772–781.
75. Ossenkoppele R, Schonhaut DR, Schöll M, et al. Tau PET patterns mirror clinical and neuroanatomical variability in Alzheimer's disease. *Brain.* 2016;139:1551–1567.
76. Vogel JW, Young AL, Oxtoby NP, et al. Four distinct trajectories of tau deposition identified in Alzheimer's disease. *Nat Med.* 2021;27:871–881.
77. Leuzy A, Smith R, Ossenkoppele R, et al. Diagnostic performance of ^{18}F-RO948 tau positron emission tomography in the differentiation of Alzheimer disease from other neurodegenerative disorders. *JAMA Neurol.* 2020;77:955–965.
78. Pascoal TA, Therriault J, Benedet AL, et al. ^{18}F-MK-6240 PET for early and late detection of neurofibrillary tangles. *Brain.* 2020;143:2818–2830.
79. Smith R, Santillo AF, Waldö ML, et al. ^{18}F-flortaucipir in TDP-43 associated frontotemporal dementia. *Sci Rep.* 2019;9:6082.
80. Mann DMA, Snowden JS. Frontotemporal lobar degeneration: pathogenesis, pathology and pathways to phenotype. *Brain Pathol.* 2017;27:723–736.
81. Ossenkoppele R, Hansson O. Towards clinical application of tau PET tracers for diagnosing dementia due to Alzheimer's disease. *Alzheimers Dement.* 2021;17: 1998–2008.
82. Johnson KA, Minoshima S, Bohnen NI, et al. Update on appropriate use criteria for amyloid PET imaging: dementia experts, mild cognitive impairment, and education. *Alzheimers Dement.* 2013;9:e106–e109.